Public Health England

NHS

NHS breast screening programme equipment report

Technical evaluation of Siemens Mammomat Inspiration digital breast tomosynthesis system − modified detector and software (VB60)

About Public Health England

Public Health England exists to protect and improve the nation's health and wellbeing, and reduce health inequalities. We do this through world-leading science, knowledge and intelligence, advocacy, partnerships and the delivery of specialist public health services. We are an executive agency of the Department of Health and Social Care, and a distinct delivery organisation with operational autonomy. We provide government, local government, the NHS, Parliament, industry and the public with evidence-based professional, scientific and delivery expertise and support.

Public Health England, Wellington House, 133-155 Waterloo Road, London SE1 8UG
Tel: 020 7654 8000 www.gov.uk/phe Twitter: @PHE_uk
Facebook: www.facebook.com/PublicHealthEngland

About PHE Screening

Screening identifies apparently healthy people who may be at increased risk of a disease or condition, enabling earlier treatment or better informed decisions. National population screening programmes are implemented in the NHS on the advice of the UK National Screening Committee (UK NSC), which makes independent, evidence-based recommendations to ministers in the 4 UK countries. The Screening Quality Assurance Service ensures programmes are safe and effective by checking that national standards are met. PHE leads the NHS Screening Programmes and hosts the UK NSC secretariat.

PHE Screening, Floor 2 Zone B, Skipton House, 80 London Road, London SE1 6LH
www.gov.uk/phe/screening
Twitter: @PHE_Screening Blog: phescreening.blog.gov.uk
Prepared by: A Mackenzie, CJ Strudley, KC Young
For queries relating to this document, please contact: phe.screeninghelpdesk@nhs.net

The image on page 9 is courtesy of Siemens.

Published December 2018
PHE publications gateway number: 2018673

PHE supports the UN Sustainable Development Goals

Acknowledgements

The authors are grateful to the staff at St George’s Hospital, Tooting, London for facilitating the evaluation of the unit at their site.

Contents

Executive summary

The technical performance of the Siemens Inspiration system with new software (VB60) was tested in tomosynthesis mode. The mean glandular dose to the standard breast (53mm thick) in tomosynthesis mode was 1.90mGy and below the reference dose level of 2.5mGy for tomosynthesis in the European Guidance. Image quality in 2D mode was comparable to previous reports for this system but appears to be improved for small detail detection in tomosynthesis mode.

Technical performance of this equipment was found to be satisfactory. This report provides baseline measurements of the equipment performance including:

- dose
- contrast detail detection
- contrast-to-noise ratio (CNR)
- reconstruction artefacts, z-resolution
- detector response
- projection modulation transfer function

1. Introduction

1.1 Testing procedures and performance standards for digital mammography

This report is one of a series evaluating commercially available mammography systems on behalf of the NHS Breast Screening Programme (NHSBSP). The testing methods and standards applied are those of the relevant NHSBSP protocols, which are published as NHSBSP Equipment Reports. Report 0604[1] covers the testing of full field digital mammography systems used for 2D imaging and Report 1407[2] covers the testing of digital breast tomosynthesis systems.

The NHSBSP protocols are similar to the European protocols,[3,4,5] but the latter also provide additional or more detailed tests and standards, some of which are included in this evaluation.

Additional tests were also carried out according to the UK recommendations for testing mammography X-ray equipment as described in IPEM Report 89.[6]

1.2 Objectives

The aims of the evaluation were:

- to conduct a limited range of measurements of technical performance of the Siemens Mammomat Inspiration system in 2D and tomosynthesis modes following a change in the detector design and software version
- to compare the performance to that given in reports for earlier versions of the Siemens Mammomat Inspiration system[7,8]
- to test the effect of warm-up time on image quality

2. Methods

2.1 System tested

Details of the system tested are given in Table 1.

Table 1. System description	
Manufacturer	Siemens Healthcare Limited
Model	Mammomat Inspiration
Detector serial number	L23-01575
Target material	Tungsten (W)
Added filtration	50µm Rhodium (Rh)
Detector type	Amorphous selenium
Detector serial number	L23-01575
Image pixel size	85µm
Detector size	240mm × 300mm
Pixel array	2800 × 3518
Source to table distance	633mm
Source to detector distance	650mm
Automatic exposure control (AEC) modes	OpDose
Tomosynthesis projections	25 equal dose projections at approximately 2° intervals from -25° to +25°
Centre of rotation	620mm from focus
Reconstructed focal planes	Focal planes at 1mm intervals, number equals compressed breast thickness plus 1 (maximum 100)
Software version	VB60

The Siemens Inspiration with software version VB30 was evaluated previously and the report was published in 2015.[7] Since then the detector has been modified and the software has been updated to version VB60. This report is limited to image quality and dose.

The system has software called PRIME which optimises the processing of 2D images taken without an anti-scatter grid but this was not tested here as it has been subject of a previous report.[8]

The system can be supplied with Siemens standard reconstruction software or Enhanced Multiple Parameter Iterative REconstruction (EMPIRE). EMPIRE was used in this report.

There is a combination mode where 2D and tomosynthesis exposures are automatically carried out during a single compression. This system also has a static mode for tomosynthesis, in which the 25 projections images are acquired with the tube at 0º. This mode was used for measuring half value layer (HVL) and tube outputs.

Siemens have a method for producing synthetic 2D images from the stack of tomosynthesis planes called Insight2D. Methods for evaluating synthetic 2D images created from the tomosynthesis planes are in development and no results are included in this report.

An image of the model tested is shown in Figure 1.

Figure 1. The Siemens Mammomat Inspiration digital breast tomosynthesis system

2.2 Dose and contrast-to-noise ratio under automatic exposure control

2.2.1 Dose measurement

Measurements were made of HVL and tube output across the clinically relevant range of kV and filter combinations for the purpose of calculating mean glandular dose (MGD) to the standard breast. Output measurements were made on the midline at the standard position, 40mm from the chest wall edge (CWE) of the breast support platform. The compression paddle was in the beam, raised well above the ion chamber.

In 2D and tomosynthesis modes, exposures of a range of thicknesses of polymethyl methacrylate (PMMA) were made under automatic exposure control (AEC). For each measurement the height of the paddle was set to match the indicated thickness to the equivalent breast thickness for that thickness of PMMA. Spacers were used to enable compression force to be applied.

MGDs to the standard breast model for the exposures were calculated using the methods described in the UK protocols.[1,2] The method of measuring tomosynthesis doses described in the UK protocol differs slightly from the method described by Dance et al.[9] The incident air kerma is measured with the compression paddle well above, instead of in contact with, the ion chamber. Measurements on other systems[7,10] show that this variation reduces the air kerma and thus the MGD measurement by 3% to 5%. Otherwise the MGDs in tomosynthesis mode were calculated using the method described by Dance et al.[7] This is an extension of the established 2D method, using the equation:

$$D = KgcsT \quad (1)$$

where *D* is the MGD (mGy), *K* is the incident air kerma (mGy) at the top surface of the PMMA blocks, and *g, c* and *s* are conversion factors. The additional factor, *T*, is derived by summing weighted correction factors for each of the tomosynthesis projections.

2.2.2 Contrast-to-noise ratio

For contrast-to-noise ratio (CNR) measurements a 10mm x 10mm square of 0.2mm thick aluminium foil was included in the phantom described above, positioned 10mm above the table on the midline, 60mm from the CWE.

For 2D images, the 5mm x 5mm regions of interest (ROI) were subdivided into 1mm x 1mm elements and the background ROIs were positioned adjacent to the aluminium square, as shown in Figure 2. The mean pixel values and their standard deviations were averaged over all the 1mm x 1mm elements, and the CNR was calculated from these averages.

The tomosynthesis focal plane CNR was measured in the focal plane in which the aluminium square was brought into focus. The tomosynthesis ROIs were placed as shown in Figure 2. The tomosynthesis CNR was calculated using the average of the mean and standard deviation of the pixel value for each 5mm x 5mm element.

CNR was also assessed in the unprocessed tomosynthesis projections acquired for the above images, using a 5mm x 5mm ROI.

The variation in central projection CNR with breast thickness and the variation in projection CNR with projection angle for a 53mm thick breast (45mm PMMA) were also assessed.

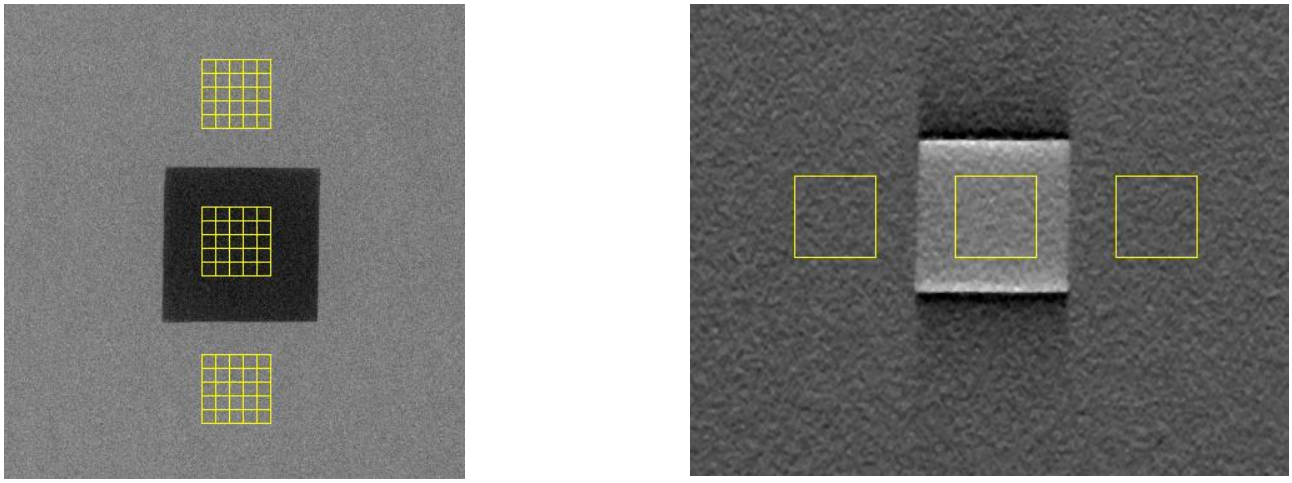

Figure 2. The positioning of 5mm x 5mm ROIs for assessment of CNR. (The CWE is to the right of the image extracts): 2D (Left) and tomosynthesis planes (Right)

It had been reported that the CNR and therefore image quality for this system improves for a time after switch on. Therefore measurements of CNR were made immediately after switch on and during the next hour.

2.3 Detector response

Detector response was measured for the detector operating in 2D and tomosynthesis (stationary tube) modes. An aluminium filter, of 2mm thickness, was placed in the beam and attached to the tube port. The compression paddle was removed. A typical beam quality was selected and images were acquired using a range of tube load settings in 2D and tomosynthesis modes. The air kerma was measured and corrected using the inverse square law to give the air kerma incident at the detector. No corrections were made for the attenuation of X-rays by the breast support. Using a 10mm x 10mm ROI positioned on the midline 50mm from the CWE of the central projection image, measurements were made of the mean pixel value, which was plotted against air kerma incident at the detector.

2.4 Noise analysis

The images acquired in the measurements of detector response using 29kV W/Rh were used to analyse the image noise. The image data was linearised by applying the inverse of the detector response to each pixel value. A small ROI with an area of approximately 2.5mm x 2.5mm was placed on the midline, 60mm from the CWE. The average standard deviations of the pixel values in these ROI for each image were used to investigate the relationship between dose to the detector and the image noise. It was assumed that this noise comprises three components; electronic noise, structural noise, and quantum noise with the relationship shown in Equation 1:

$$\sigma_p = \sqrt{k_e^2 + k_q{}^2 p + k_s{}^2 p^2} \quad (1)$$

where σ_p is the standard deviation in pixel values within an ROI with a uniform exposure and a mean pixel value p, and k_e, k_q, and k_s are the coefficients determining the amount of electronic, quantum, and structural noise in a pixel with a value p. This method of analysis has been described previously.[7] For simplicity, the noise is generally presented here as relative noise defined as in Equation 2.

$$\text{Relative noise} = \frac{\sigma_p}{p} \quad (2)$$

The variation in relative noise with mean pixel value was evaluated and fitted using Equation 3, and non-linear regression used to determine the best fit for the constants (k_e, k_q, and k_s) and their asymptotic confidence limits (using Graphpad Prism Version 7.00, Graphpad software, San Diego, California, USA, www.graphpad.com). This established whether the experimental measurements of the noise fitted this equation, and the relative proportions of the different noise components. The relationship between noise and pixel values has been found empirically to be approximated by a simple power relationship as shown in Equation 3.

$$\frac{\sigma_p}{p} = k_t p^{-n} \quad (3)$$

where k_t is a constant. If the noise were purely quantum noise the value of n would be 0.5. However the presence of electronic and structural noise means that n can be slightly higher or lower than 0.5.

The variance in pixel values within a ROI is defined as the standard deviation squared. The total variance was plotted against incident air kerma at the detector and fitted using Equation 3. Non-linear regression was used to determine the best fit for the constants and their asymptotic confidence limits.

Using the calculated constants the structural, electronic, and quantum components of the variance were estimated, assuming that each component was independently related to incident air kerma. The percentage of the total variance represented by each component was then calculated and plotted against incident air kerma at the detector.

2.5 Image quality measurements

A CDMAM phantom (Version 3.4, serial number 1022) was positioned between 2 blocks of PMMA, each of which was 20mm thick. The exposure factors used were close to those that would be selected by the AEC for an equivalent breast thickness of 60mm. Sets of 16 images were acquired at the AEC selected dose level in 2D and tomosynthesis modes.

For tomosynthesis, the image corresponding to the focal plane of the vertical position of the CDMAM phantom was extracted from each reconstructed stack of images. The 2D and tomosynthesis sets of CDMAM images were read and analysed using 2 software tools:

CDCOM version 1.6 (www.euref.org) and CDMAM Analysis version 2.1 (NCCPM, Guildford, UK). This was repeated for up to 2 focal planes immediately above and below the expected plane of best focus to ensure that the threshold gold thickness result quoted corresponded to the best image quality obtained.

In order to compare the results in this report with previous reports the MGD for 2D images was calculated at the minimum acceptable and achievable image quality levels using the following relationship.

$$T = \lambda D^{-n} \qquad (4)$$

where T is the threshold gold thickness (μm), D is the MGD for a 60mm thick standard breast equivalent to the test phantom configuration used for the image quality measurement, and λ is a constant to be fitted. It was assumed that n had a value of 0.5.

2.6 Geometric distortion and reconstruction artefacts

The relationship between reconstructed tomosynthesis focal planes and the physical geometry of the volume that they represent was assessed. This was done by imaging a geometric test phantom consisting of a rectangular array of 1mm diameter aluminium balls at 50mm intervals in the middle of a 5mm thick sheet of PMMA. The phantom was placed at various heights (7.5, 32.5, and 52.5mm) above the breast support table within a 60mm stack of plain sheets of PMMA. Reconstructed tomosynthesis planes were analysed to find the height of the focal plane in which each ball was best in focus, the position of the centre of the ball within that plane, and the number of adjacent planes in which the ball was also seen. The variation in appearance of the ball between focal planes was quantified.

This analysis was automated using a software tool developed at the National Coordinating Centre for the Physics of Mammography (NCCPM) for this purpose. This software is in the form of a plug-in for use in conjunction with ImageJ (http://rsb.info.nih.gov/ij/).

2.6.1 Height of best focus

For each ball, the height of the focal plane in which it was best in focus was identified. Results were compared for all balls within each image, to judge whether there was any tilt of the test phantom relative to the reconstructed planes, or any vertical distortion of the focal planes within the image.

2.6.2 Positional accuracy within focal plane

The x and y co-ordinates within the image were found for each ball (x and y are perpendicular and parallel to the CWE, respectively). The mean distances between adjacent balls were calculated, using the pixel spacing quoted in the DICOM image header. This was compared to the physical separation of balls within the phantom, to assess the scaling accuracy in the x and

y directions. The maximum deviations from the mean x and y separations were calculated, to indicate whether there was any discernible distortion of the image within the focal plane.

2.6.3 Appearance of the ball in adjacent focal planes

Changes to the appearance of a ball between focal planes were assessed visually.

To quantify the extent of reconstruction artefacts in focal planes adjacent to those containing the image of the balls, the reconstructed image was treated as though it were a true three dimensional volume. The software tool was used to find the z-dimension of a cuboid around each ball which would enclose all pixels with values exceeding 50% of the maximum pixel value. The method used was to re-slice the image vertically and create a composite x-z image using the maximum pixel values from all resliced x-z focal planes. A composite z-line was then created using the maximum pixel from each column of the x-z composite plane, and a full width at half maximum (FWHM) measurement in the z-direction was made by fitting a polynomial spline. All pixel values were background subtracted using the mean pixel value from around the ball in the plane of best focus. The composite z-FWHM thus calculated (which depends on the size of the ball imaged for the purpose) was used as a measure of the inter-plane resolution, or z-resolution.

2.7 Physical measurements of the detector performance

The modulation transfer function (MTF), normalised noise power spectrum (NNPS) and the detective quantum efficiency (DQE) of the system were measured. The methods used were as close as possible to those described by the International Electrotechnical Commission (IEC).[11] The radiation quality used for the measurements was adjusted by placing a uniform 2mm thick aluminium filter at the tube housing. The beam quality used was 29kV W/Rh. The test device to measure the MTF comprised a 0.8mm thick rectangle (120mm x 60mm) of stainless steel with a polished straight edge. This test device was placed directly on the breast support table, and the anti-scatter grid was removed by selecting “grid out” at the operator console. The test device was positioned to measure the MTF in 2 directions, first almost perpendicular and then almost parallel to the CWE. A 10th order polynomial fit was applied to the MTF results.

To measure the noise power spectrum the test device was removed and exposures made for a range of incident air kerma at the surface of the table. The DQE is presented as the average of measurements in the directions perpendicular and parallel to the CWE.

3. Results

3.1 Dose and contrast-to-noise ratio under AEC

The measurements of HVL and tube output are summarised in Table 2.

Table 2. HVL and tube output measurements in 2D and tomosynthesis modes

		HVL (mmAl)		Output (µGy/mAs at 1m)	
kV	Target / Filter	2D	Tomosynthesis	2D	Tomosynthesis
25	W/Rh	0.52	0.53	8.84	8.60
28	W/Rh	0.55	0.56	12.3	11.9
31	W/Rh	0.58	0.58	15.7	15.1
34	W/Rh	0.60	0.61	19.0	18.3

The MGDs for AEC exposures in 2D and tomosynthesis modes are shown in Figure 3 with the 2D remedial levels[1] and tomosynthesis reference dose levels[6].

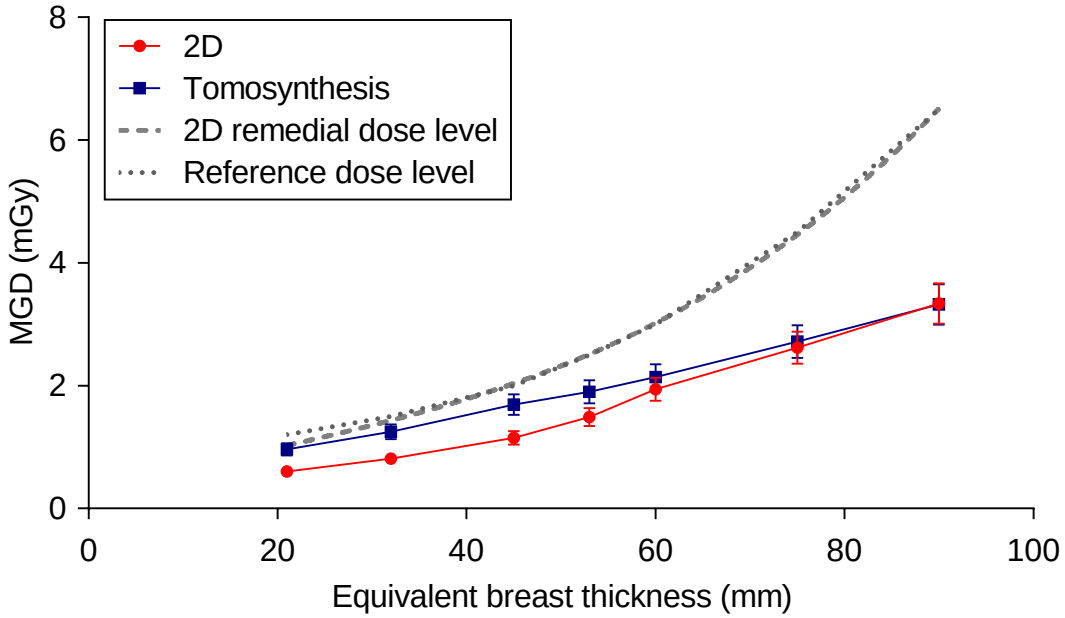

Figure 3. Mean glandular doses to the standard breast model simulated using PMMA. Error bars indicate 95% confidence limits.

The CNR measurements in 2D and in the reconstructed tomosynthesis images (focal planes) are shown in Figure 4.

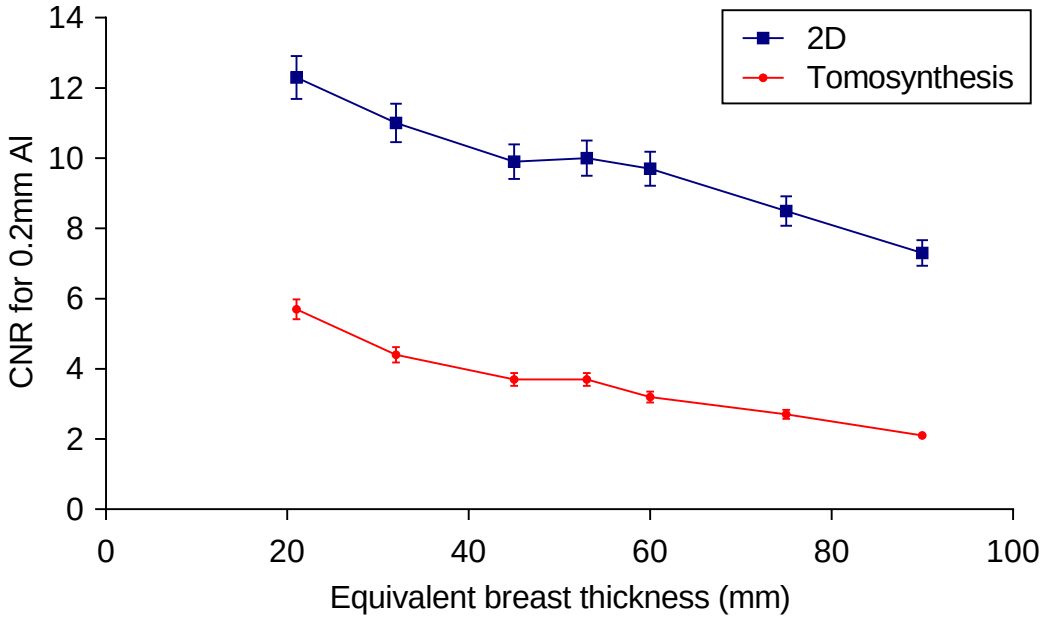

Figure 4. CNR for 2D images and tomosynthesis reconstructed planes, acquired under AEC. Error bars indicate 95% confidence limits.

The MGDs and CNRs shown in Figures 3 and 4 are listed in Table 3 (2D) and Table 4 (tomosynthesis) together with exposure factors. All MGDs quoted include the preliminary exposure which is not included in the image. Figure 5 shows the CNR in the projection images at different projection angles. The CNR required to reach the minimum acceptable and achievable image quality levels in the European protocol were 4.3 and 6.6 respectively.

Table 3. Dose and CNR for 2D images acquired under AEC

PMMA thickness (mm)	Equivalent breast thickness (mm)	kV	Target/ filter	mAs	MGD (mGy)	Remedial dose level (mGy)	CNR
20	21	26	W/Rh	43.8	0.60	1.0	12.3
30	32	27	W/Rh	64.9	0.81	1.5	11.0
40	45	28	W/Rh	97.7	1.15	2.0	9.9
45	53	29	W/Rh	124.2	1.49	2.5	10.0
50	60	30	W/Rh	155.6	1.94	3.0	9.7
60	75	31	W/Rh	217.7	2.62	4.5	8.5
70	90	32	W/Rh	295.9	3.34	6.5	7.3

Table 4. Dose and CNR for tomosynthesis reconstructed planes under AEC, images acquired under AEC

PMMA thickness (mm)	Equivalent breast thickness (mm)	kV	Target/ filter	mAs	MGD (mGy)	Reference dose level (mGy)	CNR
20	21	26	W/Rh	72.5	0.96	1.2	5.7
30	32	27	W/Rh	103.8	1.25	1.5	4.4
40	45	28	W/Rh	150.3	1.69	2.0	3.7
45	53	29	W/Rh	165.5	1.90	2.5	3.7
50	60	30	W/Rh	180.8	2.14	3.0	3.2
60	75	31	W/Rh	242.6	2.72	4.5	2.7
70	90	32	W/Rh	311.4	3.32	6.5	2.1

Figure 5 shows the CNR in the projection images at different projection angles. It shows the typical fall off of CNR at oblique angles.

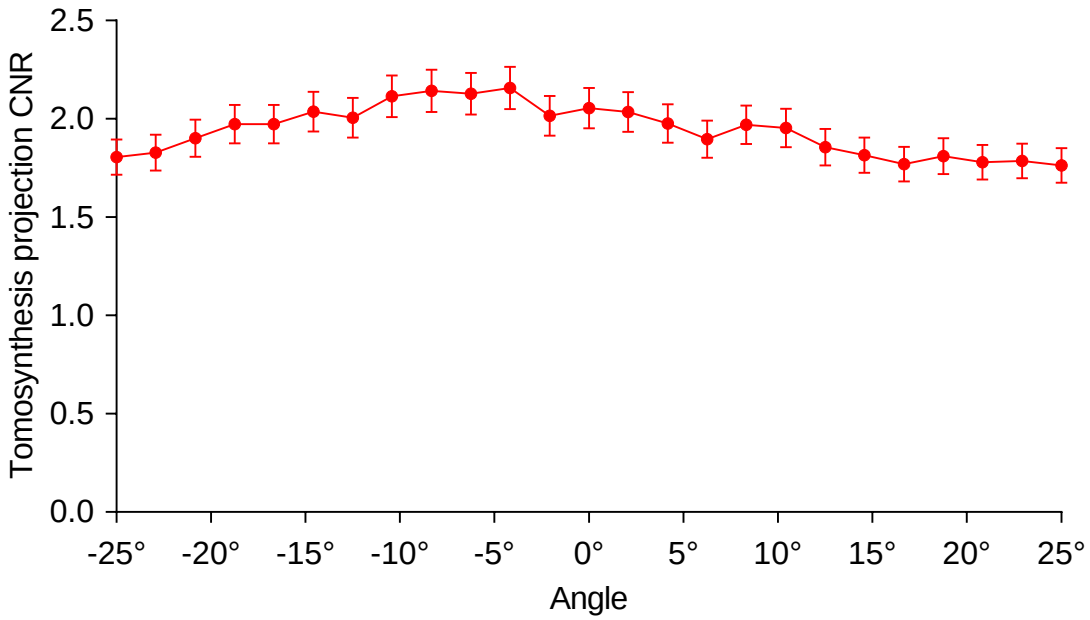

Figure 5. Variation of projection CNR with angle with 45mm PMMA. Error bars indicate 95% confidence limits.

3.2 Detector response

The detector response for 2D and for the first projection of the tomosynthesis images acquired at 29kV W/Rh are shown in Figures 6a and 6b.

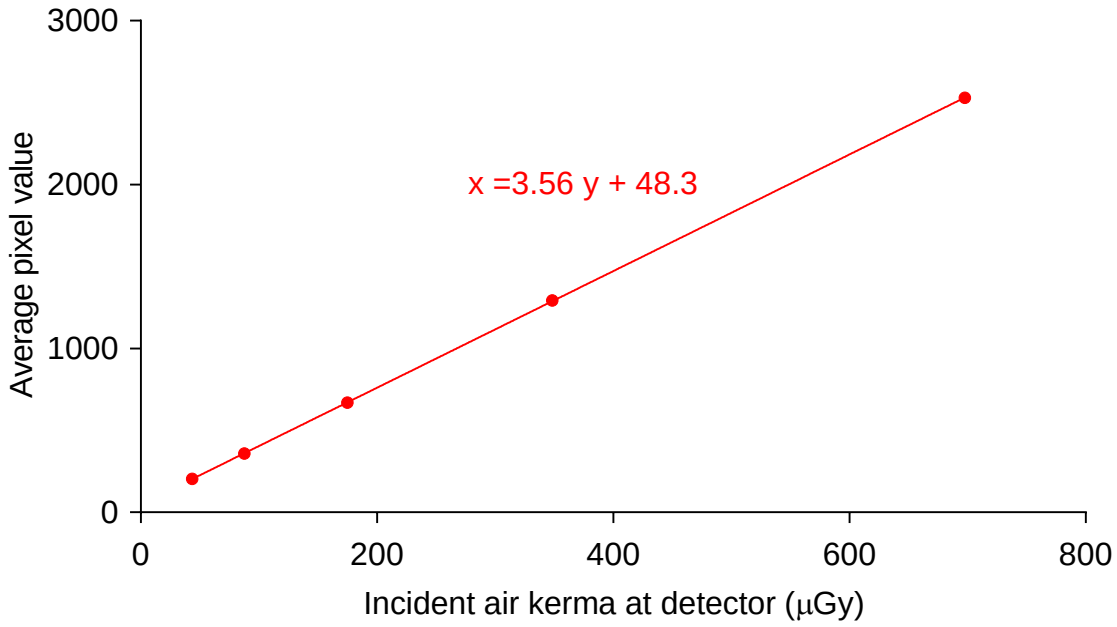

Figure 6a. Detector response in 2D mode

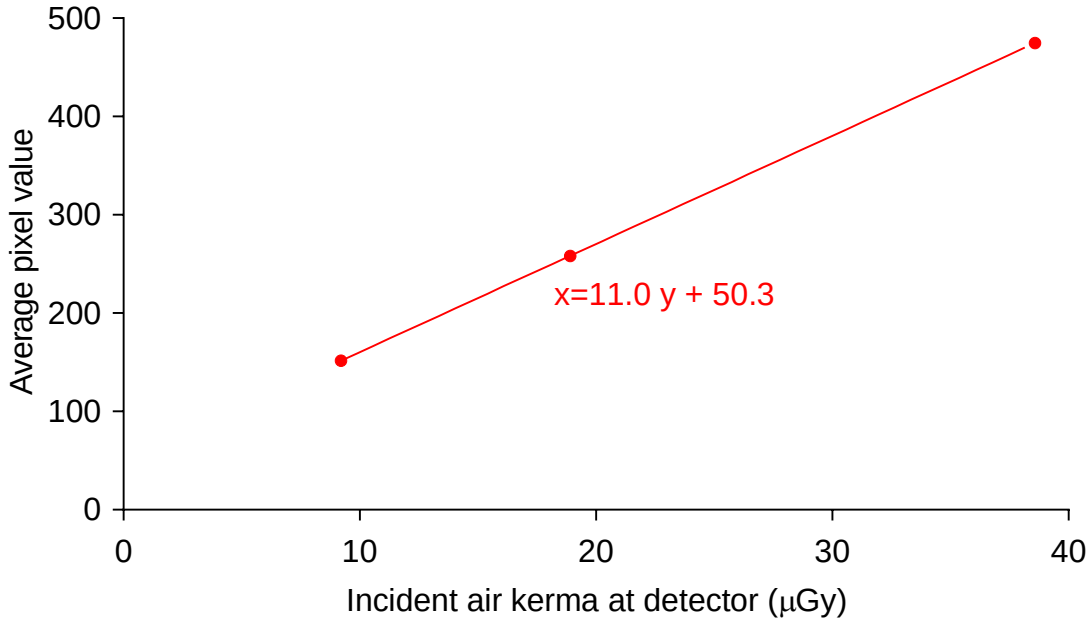

Figure 6b. Detector response of the first projection image in tomosynthesis mode

3.3 Noise measurements

The variation in noise with dose for 2D images was analysed by plotting the standard deviation in linearised pixel values against the detector entrance air kerma, as shown in Figure 7. The fitted power curve has an index close to 0.50, which is the expected value for quantum noise sources alone.

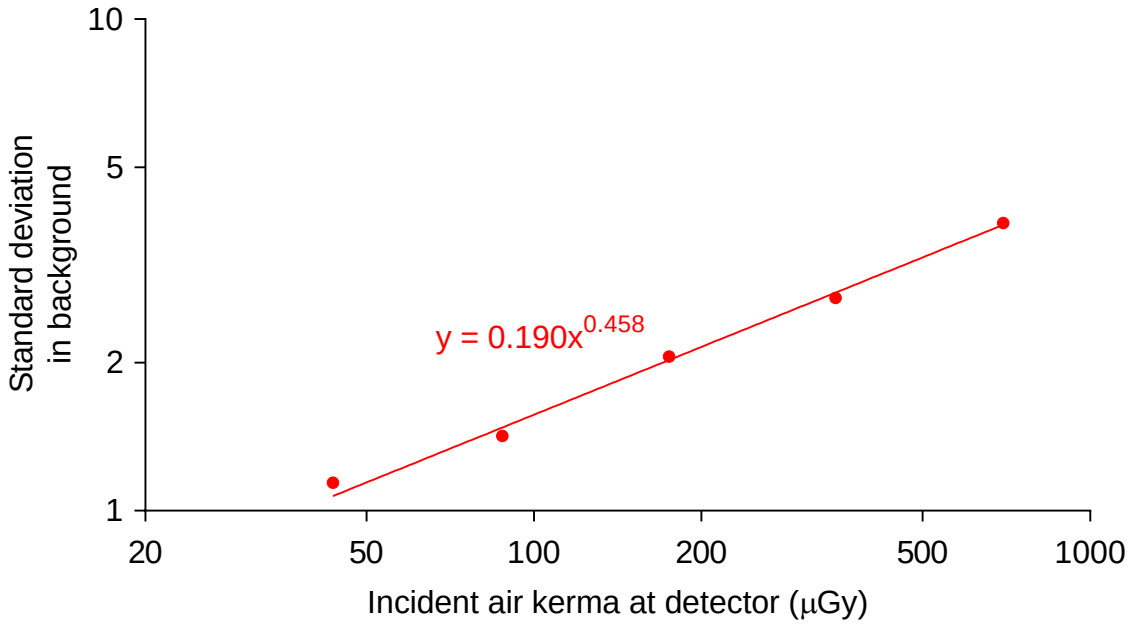

Figure 7. Standard deviation of linearized pixel values versus air kerma at detector

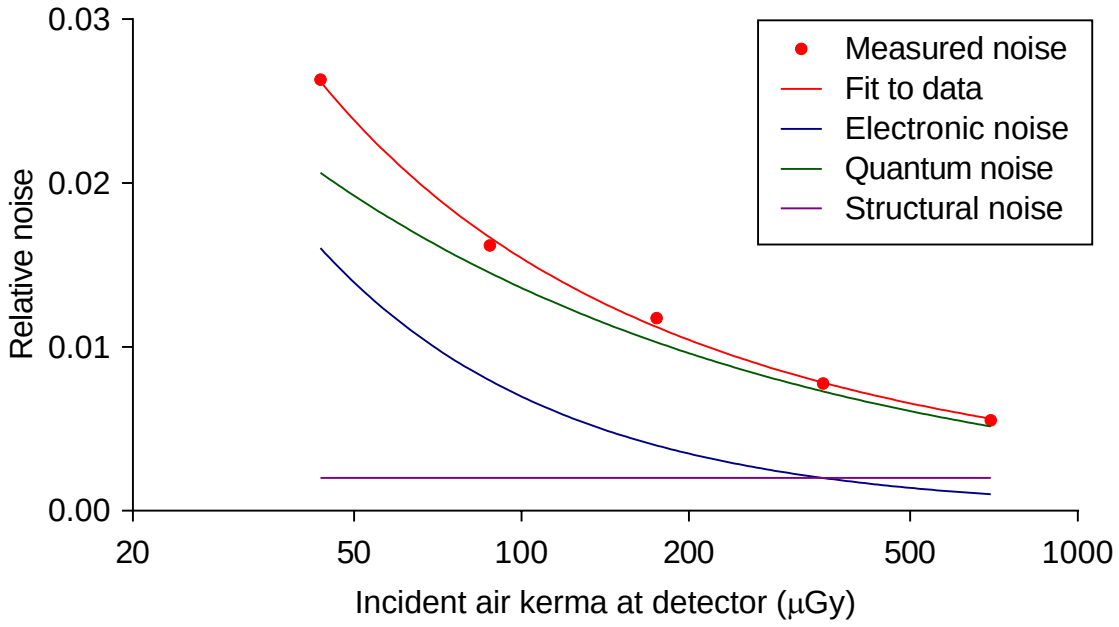

Figure 8. Relative noise and noise components

Figure 8 shows the relative noise at different incident air kerma. The estimated relative contributions of electronic, structural, and quantum noise are shown and the quadratic sum of these contributions fitted to the measured noise (using Equation 3).

Figure 11 shows the different amounts of variance due to each component. The quantum noise is the dominant noise source for all incident air kerma.

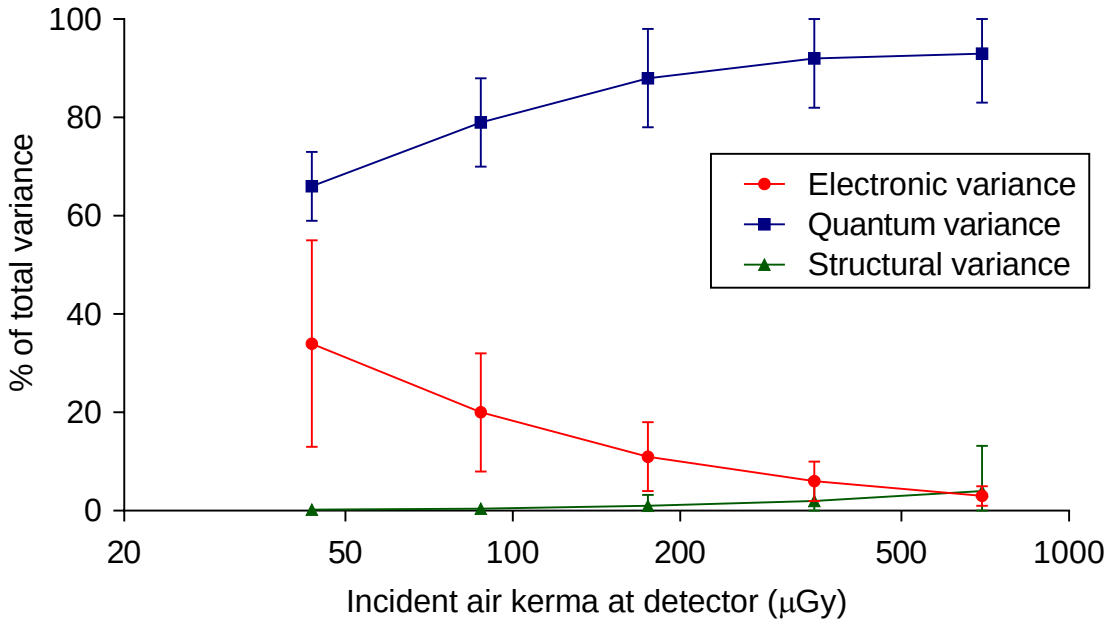

Figure 9. Noise components as a percentage of the total variance. Error bars indicate 95% confidence limits.

3.4 Image quality measurements

Figure 10 shows the contrast detail curves for the 2D images and the tomosynthesis focal plane which has the CDMAM best in focus. The threshold gold thicknesses were lowest for focal plane 26. Table 5 summarises the image quality measurements for 2D and tomosynthesis modes. The doses required to meet the minimum acceptable and achievable image quality levels, in 2D mode, are shown for this and a previous report in Table 6.

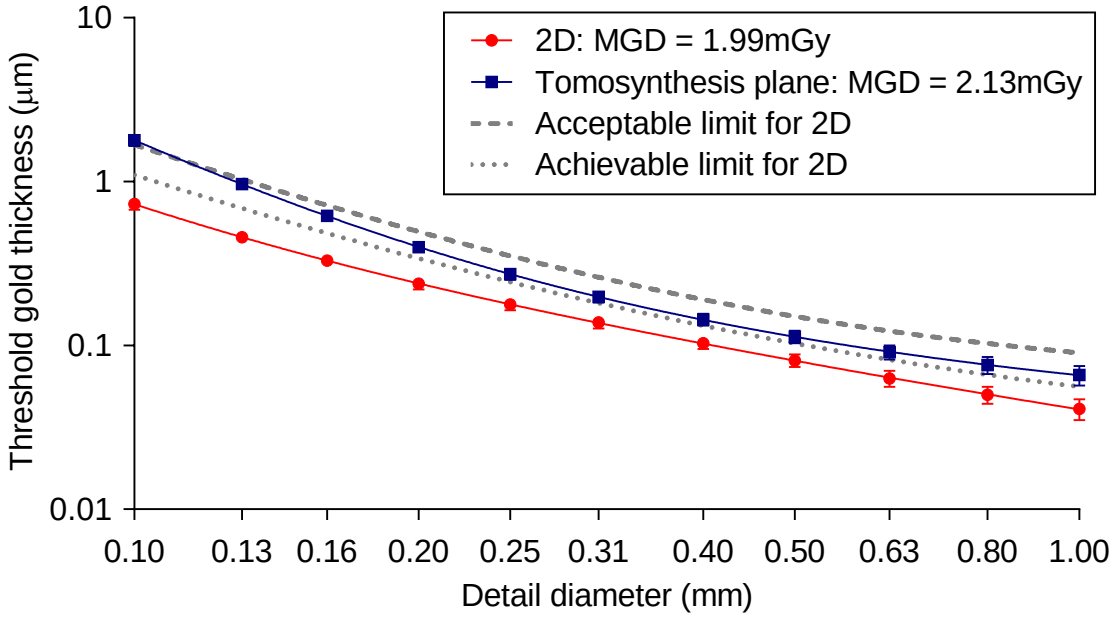

Figure 10. Threshold gold thickness detail curves for 2D and reconstructed focal planes. Error bars indicate 95% confidence limits.

Table 5. Threshold gold thickness for 2D and reconstructed focal plane 26 (fit to predicted human data).

Detail diameter (mm)	Threshold gold thickness (µm)			
	Acceptable	Achievable	2D (1.99mGy)	Tomosynthesis (2.13mGy)
0.1	1.680	1.100	0.73 ± 0.06	1.79 ± 0.14
0.25	0.352	0.244	0.178 ± 0.014	0.27 ± 0.02
0.5	0.150	0.103	0.081 ± 0.007	0.11 ± 0.01
1.0	0.091	0.056	0.041 ± 0.006	0.066 ± 0.009

Table 6. The MGD for a 60mm equivalent breast for different systems to reach the minimum and achievable threshold gold thicknesses for 0.1 and 0.25 mm details (2D images).

System	Minimum acceptable		Achievable	
	MGD (mGy) for 0.1mm	MGD (mGy) for 0.25mm	MGD (mGy) for 0.1mm	MGD (mGy) for 0.25mm
Siemens Inspiration (Report 1503)	0.54 ± 0.11	0.55 ± 0.11	1.16 ± 0.08	1.06 ± 0.10
Siemens Inspiration (This report with VB60 software)	0.38 ± 0.08	0.55 ± 0.11	0.88 ± 0.18	1.06 ± 0.21

3.5 Geometric distortion and resolution between focal planes

3.5.1 Height of best focus

For each of the 3 images of the phantom acquired at different heights, the height of best focus for each ball was found to increase with distance from the CWE. The sharpest images of spheres furthest from the CWE were 2mm higher than the nearest ones. This indicates that the reconstructed focal planes are aligned to the horizontal plane rather than to the slightly inclined surface of the breast support table. At the CWE the height of best focus for each ball was found to be within 1mm of its height above the table. For each set of balls at the same distance from the CWE the height variation was no greater than 1mm, indicating that the focal planes are flat and horizontal.

The system reconstructs 1 plane below the breast support. The number of focal planes reconstructed is equal to the indicated breast thickness in mm plus 1.

It would be possible to use small spacers below the PMMA block to make the array of spheres parallel to the reconstructed plane.

3.5.2 Positional accuracy within focal plane

No significant distortion or scaling error was seen within focal planes. Scaling errors in both the x and y directions, were found to be less than 0.5%. The maximum deviation from the average distance between the balls was 0.43mm in the x and y direction, compared to the manufacturing tolerance of 0.1mm in the positioning of each ball. If the row furthest from the chest wall was excluded then the maximum error was 0.30mm.

3.5.3 Appearance of the ball in adjacent focal planes

In the plane of best focus the balls appeared well defined and circular. When viewing successive planes, moving away from the plane of best focus, the images of the balls faded and stretched in the direction parallel to the CWE of the image. The changing appearance of one of the aluminium balls through successive focal planes is shown in Figure 11.

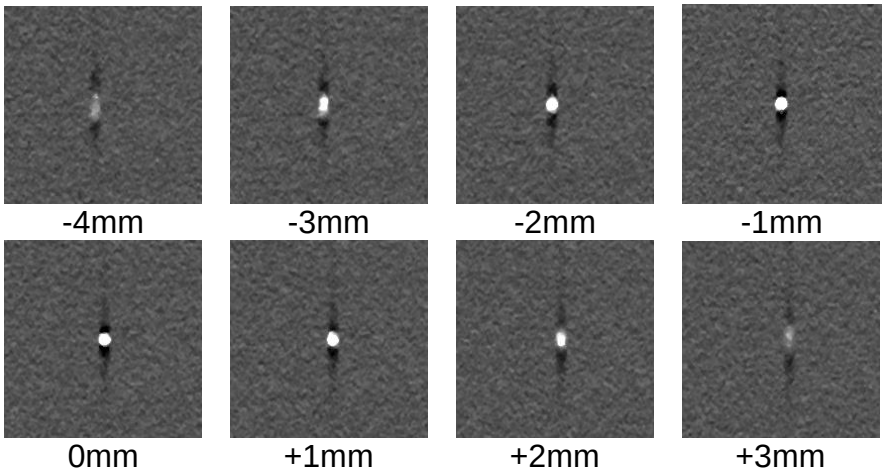

Figure 11. Appearance of 1mm aluminium balls in reconstructed focal planes at 1mm intervals from 4mm below to 3mm above the plane of best focus

Image extracts for a ball positioned in the central area, 120mm from the chest wall, are shown in Figure 12. In these images, pixels within the focal plane represent dimensions of approximately 0.085mm x 0.085mm. The spacing of reconstructed focal planes is 1mm.

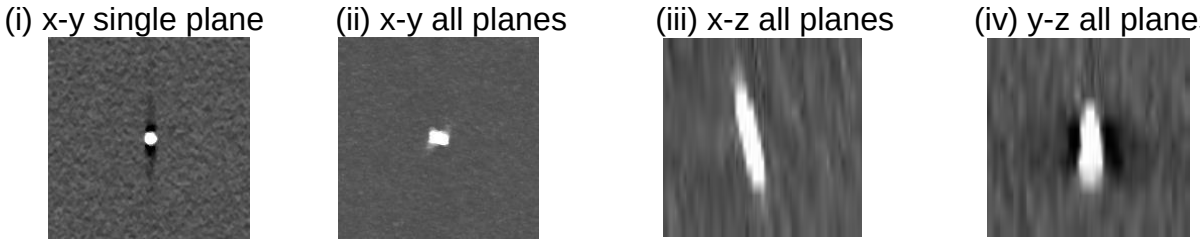

Figure 12. Extracts from planes showing 1mm aluminium ball in (i) single focal plane, (ii) the maximum intensity projections through all focal planes, and through re-sliced vertical planes in the directions (iii) parallel and (iv) perpendicular to the chest wall.

Measurements of the z-FWHM of the reconstruction artefact associated with each ball are summarised in Table 7 for images of balls at heights of 7.5mm, 32.5mm and 52.5mm above the breast support table.

Table 7. z-FWHM measurements of 1mm diameter aluminium balls

	z-FWHM (range)
Planes	7.1mm (6.2 to 9.2)

3.6 Detector performance in 2D imaging

The MTF for the central projection images is shown in Figure 13. Results are shown in the 2 orthogonal directions parallel (u) and perpendicular (v) to the tube axis. These results are summarised in Table 8. Figure 14 shows the NNPS curves for a range of entrance air kerma.

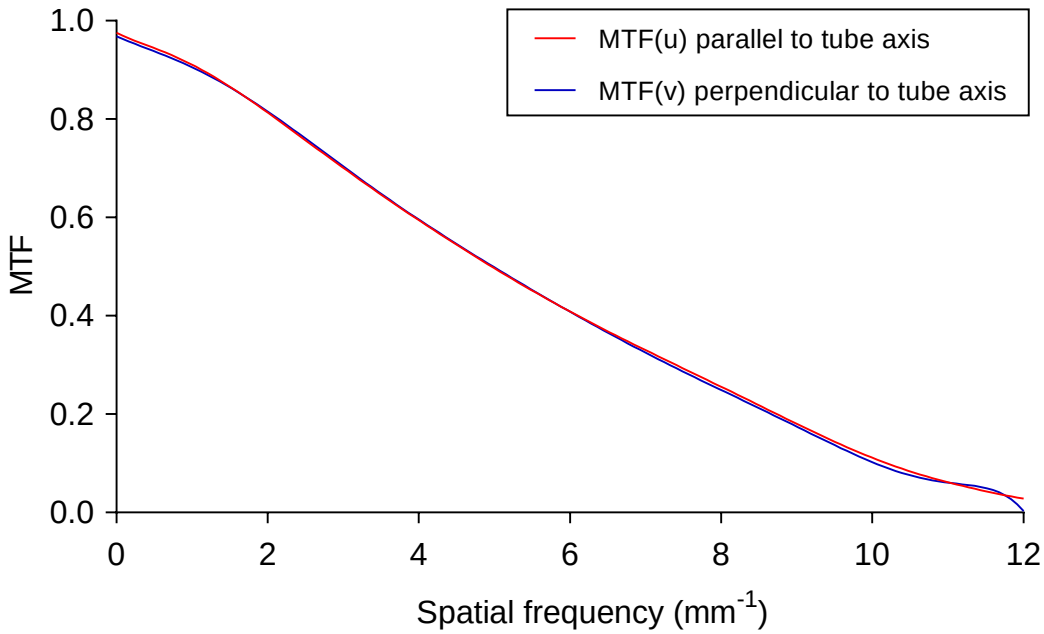

Figure 13. Pre-sampled MTF for u and v directions

The MTF50% are 4.94mm^{-1} and 4.93mm^{-1} for the u and v axes respectively.

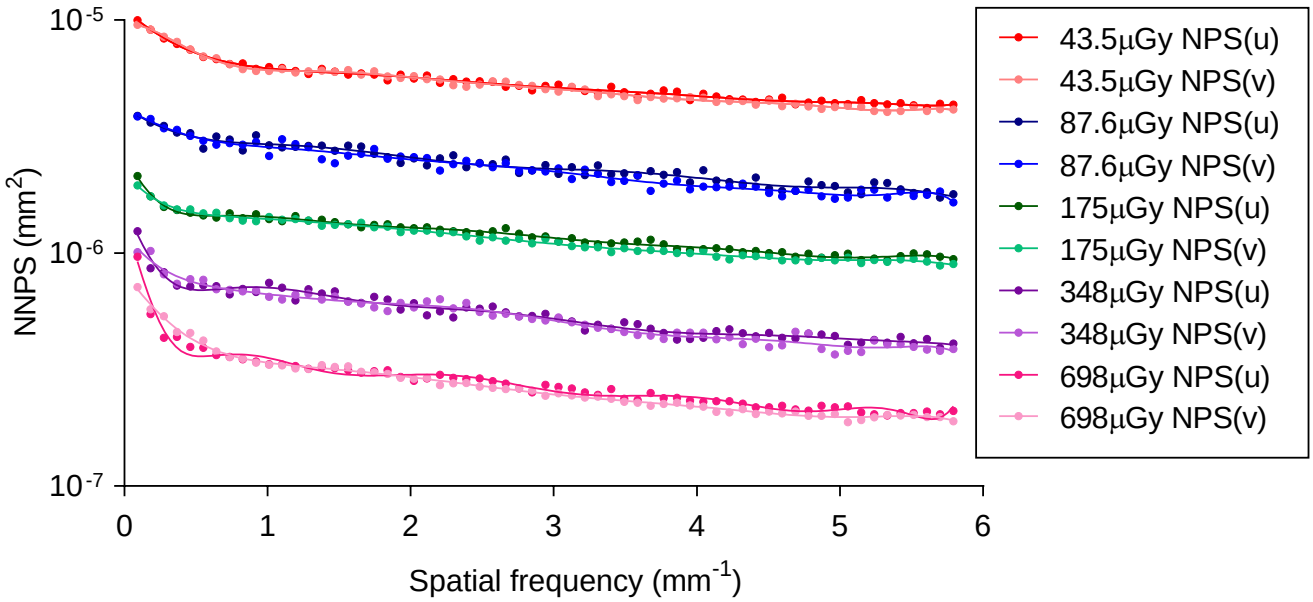

Figure 14. NNPS curves for a range of entrance air kerma for 2D images

Figure 15 shows the DQE averaged in the 2 orthogonal directions for a range of entrance air kerma. The MTF and DQE measurements were interpolated to show values at standard frequencies in Table 8.

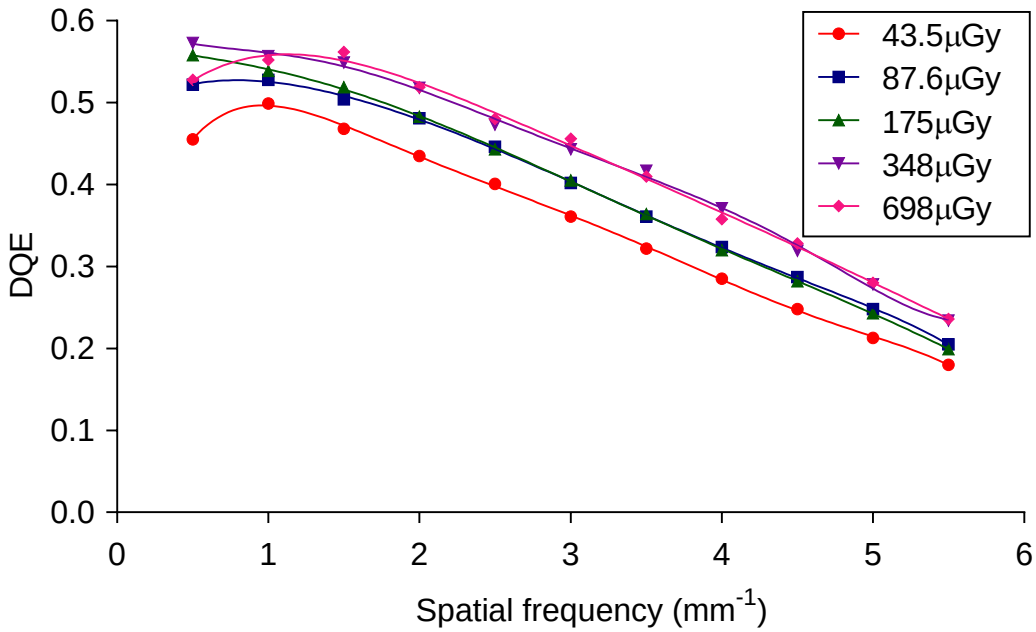

Figure 15. DQE averaged in both directions for a range of incident air kerma

Table 8. MTF and DQE measurements at standard frequencies for 2D (DQE at incident air kerma of 87.6µGy)

Frequency (mm^{-1})	Average MTF	DQE
0.0	1.00	-
0.5	0.94	0.52
1.0	0.91	0.53
1.5	0.87	0.50
2.0	0.81	0.48
2.5	0.76	0.45
3.0	0.70	0.40
3.5	0.65	0.36
4.0	0.60	0.32
4.5	0.55	0.29
5.0	0.50	0.25
5.5	0.45	0.21

3.7 Detector warm-up

Table 9 shows the CNR measured at intervals after switching the system on.

Table 9. CNR for 2D images acquired shortly after the system was switched on

Time (min)	PMMA thickness	Equivalent breast thickness	kV	Target/ filter	mAs	MGD (mGy)	CNR

	(mm)	(mm)					
0	40	45	28	W/Rh	78	0.91	7.5
28	40	45	28	W/Rh	78	0.91	7.7
43	40	45	28	W/Rh	78	0.91	8.0

Over the period of the test the CNR was seen to increase by 7%.

4. Discussion

4.1 Dose and contrast-to-noise ratio

The MGDs calculated for 2D and tomosynthesis images were within the respective remedial and reference levels set in the guidance documents.[1,5]

CNR showed a steady decrease with increasing breast thickness, for both 2D and tomosynthesis imaging.

4.2 Noise measurements

The noise contributions were measured in 2D mode. The electronic noise contributed 34% of the noise at the lowest air kerma measured. This effect is reflected in a reduced DQE for the lowest air kerma incident to the detector.

4.3 Image quality

Higher image quality in 2D mode was measured compared to previous reports, but using higher doses. When the effect of differences in dose was taken into account there were no significant differences in image quality at the 0.25mm diameter size (Table 6). The improved image quality at the 0.1mm diameter disk may not be significant as the errors in measurement are greater at this size. Nonetheless the setting of higher doses on installation of this system will lead to measurable improvements in image quality.

In the absence of any better test object for assessing tomosynthesis imaging performance, images of the CDMAM test object were acquired in tomosynthesis mode. At the AEC dose level for a 60mm equivalent breast, the threshold gold thicknesses for reconstructed focal planes is better than the minimum acceptable level and, for detail diameters greater than 0.13mm, was close to the achievable level of image quality that is applied to 2D mammography. The results were better than those for the VB30 software.

These results take no account of the ability of tomosynthesis to remove the obscuring effects of overlying tissue in a clinical image, and the degree of this effect is expected to vary between tomosynthesis systems. A standard test object that would allow a realistic and quantitative comparison of tomosynthesis image quality between systems or between 2D and tomosynthesis modes is not yet available. A suitable test object would need to incorporate simulated breast tissue to show the benefit of removing overlying breast structure in tomosynthesis imaging, as compared to 2D imaging.

4.4 Geometric distortion and reconstruction artefacts

The breast support is at a small angle relative to the horizontal and as a result the reconstructed planes were not parallel to the breast support.

The reconstructed tomosynthesis volume was found to start at approximately the level of the surface of the breast support table and continue to 1mm above the nominal height of the compression paddle. There is a maximum of 100 planes, and so any part of the object above this height is not reconstructed.

The mean inter-plane resolution (z-FWHM) for the 1mm diameter balls was 7.1mm.

4.5 Quantitative measurements

The MTF and DQE measurements were satisfactory. The MTF50% was 4.94mm^{-1} and the MTF was similar in both the x and y directions. The peak DQE was measured to be 57% for an incident air kerma of 348µGy.

5. Conclusions

The technical performance of the Siemens Mammomat Inspiration digital breast tomosynthesis system was tested in 2D and tomosynthesis modes. The performance appears to be satisfactory, though image quality standards have not yet been established for tomosynthesis systems.

The VB60 software shows improved image quality measurements for small detail detection in tomosynthesis mode, compared with that measured previously.

MGDs to the standard breast in 2D and tomosynthesis modes were found to be within the remedial and reference dose levels respectively. MGD to a 53mm thick standard breast was 1.49mGy in 2D mode and 1.90mGy in tomosynthesis mode.

This system reconstructs a maximum of 100 planes and so images of any part of the object or breast being imaged above 100mm is not reconstructed.

References

1. Workman A, Castellano I, Kulama E et al. Commissioning and Routine Testing of Full Field Digital Mammography Systems (NHSBSP Equipment Report 0604 Version 3). Sheffield: NHS Cancer Screening Programmes, 2009

2. Burch A, Loader R, Rowberry B et al. Routine quality control tests for breast tomosynthesis (physicists) (NHSBSP Equipment Report 1407). London: Public Health England, 2015

3. van Engen R, Young KC, Bosmans H et al. The European protocol for the quality control of the physical and technical aspects of mammography screening. In: European Guidelines for Quality Assurance in Breast Cancer Screening and Diagnosis, 4th Edition. Luxembourg: European Commission, 2006

4. van Engen R, Bosmans H, Dance D et al. Digital mammography update: European protocol for the quality control of the physical and technical aspects of mammography screening. In: European guidelines for quality assurance in breast cancer screening and diagnosis, Fourth edition – Supplements. Luxembourg: European Commission, 2013

5. van Engen RE, Bosmans H, Bouwman RW et al. Protocol for the Quality Control of the Physical and Technical Aspects of Digital Breast Tomosynthesis Systems. Version 1.03. www.euref.org, 2018

6. Moore AC, Dance DR, Evans DS et al. *The Commissioning and Routine Testing of Mammographic X-ray Systems.* York: Institute of Physics and Engineering in Medicine, Report 89, 2005

7. Strudley CJ, Warren LM, Young KC. Technical evaluation of Siemens Mammomat Inspiration digital breast tomosynthesis system (NHSBSP Equipment Report 1306). Sheffield: NHS Cancer Screening Programmes, 2015

8. Oduko JM, Strudley CJ, Young KC. Technical evaluation of Siemens Inspiration PRIME with VB30L software (NHSBSP Equipment Report 1503). Sheffield: NHS Cancer Screening Programmes, 2015

9. Dance DR, Young KC, van Engen RE. Estimation of mean glandular dose for breast tomosynthesis: factors for use with the UK, European and IAEA breast dosimetry protocols. Physics in Medicine and Biology, 2011, 56: 453-471.

10. Strudley CJ, Looney P, Young KC. Technical evaluation of Hologic Selenia Dimensions digital breast tomosynthesis system (NHSBSP Equipment Report 1307 Version 2). Sheffield: NHS Cancer Screening Programmes, 2014.

11. IEC 62220-1-2, *Determination of the detective quantum efficiency – Detectors used in mammography.* International Electrotechnical Commission, 2007